A New Capacity Scaling Law in Ultra-Dense Networks

Ming Ding[‡], David López Pérez[†], Guoqiang Mao[♯‡]
[‡]*Data61, Australia* {Ming.Ding@data61.csiro.au}
[†]*Nokia Bell Labs, Ireland* {david.lopez-perez@nokia.com}
[♯]*School of Computing and Communication, University of Technology Sydney, Australia*

arXiv:1704.00399v1 [cs.NI] 3 Apr 2017

***Abstract*—We discover a new capacity scaling law in ultra-dense networks (UDNs) under practical system assumptions, such as a general multi-piece path loss model, a non-zero base station (BS) to user equipment (UE) antenna height difference, and a finite UE density. The intuition and implication of this new capacity scaling law are completely different from that found in year 2011. That law indicated that the increase of the interference power caused by a denser network would be exactly compensated by the increase of the signal power due to the reduced distance between transmitters and receivers, and thus network capacity should grow *linearly* with network densification. However, we find that both the signal and interference powers become bounded in practical UDNs, which leads to a *constant* capacity scaling law. As a result, network densification should be *stopped* at a certain level for a given UE density, because the network capacity will reach its limit due to *(i)* the bounded signal and interference powers, and *(ii)* a finite frequency reuse factor because of a finite UE density. Our new discovery on the *constant* capacity scaling law also resolves the recent concerns about network capacity collapsing in UDNs, e.g., the capacity crash due to a non-zero BS-to-UE antenna height difference, or a bounded path loss model of the near-field (NF) effect, etc.**

I. Introduction

Orthogonal deployments of dense small cell networks (SCNs), in which small cells and macrocells operate in different frequency bands (i.e., the 3rd Generation Partnership Project (3GPP) SCN Scenario #2a in [1]), have been identified as one of the most promising approaches to rapidly increase network capacity in the 4th-generation (4G) and the 5th-generation (5G) systems [2]. In this paper, we focus on the analysis of these dense SCNs as they go ultra-dense (UD) in 5G, a.k.a. ultra-dense networks (UDNs), and shed new light on their capacity scaling law.

Before 2015, the common understanding on these UDNs was that the density of base stations (BSs) would not affect the per-BS coverage probability performance in an interference-limited[1] and fully-loaded[2] wireless network [4], where the coverage probability is defined as the probability that the signal-to-interference-plus-noise ratio (SINR) of a typical user equipment (UE) is above a SINR threshold γ. Such phenomenon is referred to as the SINR invariance and is shown in Fig. 1. The intuition of such conclusion is that the increase in the interference power caused by a denser network would be exactly compensated by the increase in the signal power due to the reduced distance between transmitters and receivers [4]. Consequently, network capacity should scale *linearly* as the BS density increases in a fully-loaded UDN.

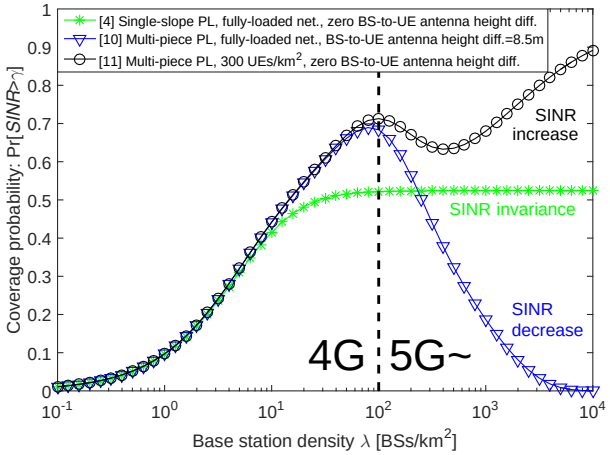
[4] Single-slope PL, fully-loaded net., zero BS-to-UE antenna height diff.
[10] Multi-piece PL, fully-loaded net., BS-to-UE antenna height diff.=8.5m
[11] Multi-piece PL, 300 UEs/km^2, zero BS-to-UE antenna height diff.
SINR increase
SINR invariance
SINR decrease
4G
5G~
Coverage probability: Pr[SINR>γ]
Base station density λ [BSs/km^2]

Fig. 1. Theoretical performance comparison of the coverage probability when the SINR threshold $\gamma = 0$ dB. Note that all the results are obtained using practical 3GPP channel models [5], which will be introduced in details later. Moreover, the BS density regions for the 4G and 5G networks have been illustrated in the figure, considering that the maximum BS density of a 4G SCN is in the order of 100 BSs/km^2 [1].

Such conclusion, however, was obtained with considerable simplifications on network conditions and propagation environment. Recently, a few noteworthy studies have followed and revisited the network performance analysis of UDNs using more practical assumptions [6–11], such as

- a general multi-piece path loss model with probabilistic line-of-sight (LoS) and non-LoS (NLoS) transmissions,
- a non-zero BS-to-UE antenna height difference L, and
- a non-fully-loaded network with a finite UE density ρ.

The inclusion of these more realistic assumptions significantly changed the previous conclusion on *the SINR invariance* [4], indicating that the coverage probability performance of UDNs is *neither a convex nor a concave function* with respect to the BS density. In particular, two seemingly contradictory performance behaviors have been discovered in [10] and [11], both considering a general multi-piece path loss model recommended by the 3GPP.

[1]In an interference-limited network, the power of each BS is set to a value much larger than the noise power.

[2]In a fully-loaded network, all BSs are active. Such assumption implies that the user density is infinity or much larger than the BS density. According to the results in [3], the user density should be at least 10 times higher than the BS density to make sure that almost all BSs are active.

First, if we consider a practical non-zero BS-to-UE antenna height difference L, then the coverage probability is shown to crash as the BS density increases in 5G. This is caused by a severe *SINR decrease* in UDNs [10], as exhibited in Fig. 1 with $L = 8.5\,\text{m}$, where the SCN BS antenna height and the UE antenna height are assumed to be 10 m and 1.5 m, respectively [5]. The intuition of such *SINR decrease* is that the signal power becomes bounded in UDNs due to the lower-bound L on the BS-to-UE distance.

Second, if we consider a practical finite UE density ρ, then the coverage probability is shown to take off as the BS density increases in 5G. This is caused by a soaring *SINR increase* in UDNs [11], as exhibited in Fig. 1 with a UE density of $\rho = 300\,\text{UEs/km}^2$, where this is a typical UE density in populated scenarios in 5G [2]. The intuition of such *SINR increase* is that the interference power becomes bounded in UDNs due to the partial activation of a finite density of BSs to serve a finite density of UEs ρ. In more detail, a large number of BSs can switch off their transmission modules in an UDN, entering into idle mode, if there is no active UE within their coverage areas, and as a result, the number of interfering BSs is determined by the number of finite UEs.

Considering that the above two seemingly contradictory performance behaviors (i.e., *SINR decrease* and *increase*) manifest themselves in UDNs, an intriguing question rises: *What occurs in reality when both effects are considered? Which one prevails in UDNs?* In this paper, we answer this fundamental question by theoretical analyses. In particular,

- **We present and prove the existence of a new SINR invariance in UDNs under practical assumptions.**
- **Then, we discover and prove a new capacity scaling law in UDNs, which is a constant scaling law.**

II. Network Scenario and System Model

In this section, we present the network scenario and the wireless system model considered in this paper.

A. Network Scenario

We consider a downlink (DL) cellular network with BSs deployed on a plane according to a homogeneous Poisson point process (HPPP) Φ with a density of λ BSs/km^2. Active DL UEs are also Poisson distributed in the considered network with a density of ρ UEs/km^2. Here, we only consider active UEs in the network because non-active UEs do not trigger any data transmission. As indicated earlier [2], a typical UE density in populated scenarios in 5G is around $\rho = 300\,\text{UEs/km}^2$.

In practice, a BS will enter into idle mode, if there is no UE connected to it, which reduces the interference to UEs in neighboring BSs as well as the energy consumption of the network. Since UEs are randomly and uniformly distributed in the network, the active BSs should follow another HPPP distribution $\tilde{\Phi}$ [3], the density of which is $\tilde{\lambda}$ BSs/km^2. Note that $\tilde{\lambda} \leq \lambda$ and $\tilde{\lambda} \leq \rho$, since one UE is served by at most one BS. Also note that a larger ρ results in a larger $\tilde{\lambda}$.

From [3, 11], $\tilde{\lambda}$ is given by

$$\tilde{\lambda} = \lambda \left[1 - \frac{1}{\left(1 + \frac{\rho}{q\lambda}\right)^q} \right], \tag{1}$$

where an empirical value of 3.5 was suggested for q in [3].

B. Wireless System Model

The two-dimensional (2D) distance between a BS and an a UE is denoted by r. Moreover, the absolute antenna height difference between a BS and a UE is denoted by L. Thus, the 3D distance between a BS and a UE can be expressed as

$$w = \sqrt{r^2 + L^2}. \tag{2}$$

Note that the value of L is in the order of several meters [5].

Following [8], we adopt a general path loss model, where the path loss $\zeta(w)$ is a multi-piece function of w written as

$$\zeta(w) = \begin{cases} \zeta_1(w), & \text{when } 0 \leq w \leq d_1 \\ \zeta_2(w), & \text{when } d_1 < w \leq d_2 \\ \vdots & \vdots \\ \zeta_N(w), & \text{when } w > d_{N-1} \end{cases}, \tag{3}$$

where each piece $\zeta_n(w), n \in \{1, 2, \ldots, N\}$ is modeled as

$$\zeta_n(w) = \begin{cases} \zeta_n^{\text{L}}(w) = A_n^{\text{L}} w^{-\alpha_n^{\text{L}}}, & \text{LoS: } \Pr_n^{\text{L}}(w) \\ \zeta_n^{\text{NL}}(w) = A_n^{\text{NL}} w^{-\alpha_n^{\text{NL}}}, & \text{NLoS: } 1 - \Pr_n^{\text{L}}(w) \end{cases}, \tag{4}$$

where

- $\zeta_n^{\text{L}}(w)$ and $\zeta_n^{\text{NL}}(w), n \in \{1, 2, \ldots, N\}$ are the n-th piece path loss functions for the LoS and the NLoS cases, respectively,
- A_n^{L} and A_n^{NL} are the path losses at a reference 3D distance $w = 1$ for the LoS and the NLoS cases, respectively,
- α_n^{L} and α_n^{NL} are the path loss exponents for the LoS and the NLoS cases, respectively.

Moreover, $\Pr_n^{\text{L}}(w)$ is the n-th piece LoS probability function that a transmitter and a receiver separated by a 3D distance w has a LoS path, which is assumed to be *a monotonically decreasing function* with respect to w. Existing measurement studies have confirmed this assumption [5].

As a special case to show our analytical results in the following sections, we consider a practical two-piece path loss function and a two-piece exponential LoS probability function, defined by the 3GPP [5]. Specifically, we have $N = 2$, $\zeta_1^{\text{L}}(w) = \zeta_2^{\text{L}}(w) = A^{\text{L}} w^{-\alpha^{\text{L}}}$, $\zeta_1^{\text{NL}}(w) = \zeta_2^{\text{NL}}(w) = A^{\text{NL}} w^{-\alpha^{\text{NL}}}$, $\Pr_1^{\text{L}}(w) = 1 - 5\exp(-R_1/w)$, and $\Pr_2^{\text{L}}(w) = 5\exp(-w/R_2)$, where $R_1 = 156$ m, $R_2 = 30$ m, and $d_1 = \frac{R_1}{\ln 10} = 67.75$ m [5]. For clarity, this case is referred to as **the 3GPP Case** hereafter. Note that **the 3GPP Case** has been used to generate the results in Fig. 1 of Section I.

Furthermore, we assume a practical user association strategy (UAS), in which each UE is connected to the BS giving the maximum average received signal strength (i.e., with the largest $\zeta(w)$) [7, 8]. Finally, we assume that each BS's transmission power is a constant value P, each BS/UE is equipped with an isotropic antenna, and the multi-path fading

Theorem 1. *Considering the general path loss model in (3) and the adopted UAS,* $\lim_{\lambda\to+\infty} p^{cov}(\lambda,\gamma)$ *can be derived as*

$$\lim_{\lambda\to+\infty} p^{cov}(\lambda,\gamma)=\lim_{\lambda\to+\infty}\Pr\left[\frac{P\zeta_1^{\mathrm{L}}(L)\,h}{I_{\mathrm{agg}}+P_{\mathrm{N}}}>\gamma\right]=\exp\left(-\frac{P_{\mathrm{N}}\gamma}{P\zeta_1^{\mathrm{L}}(L)}\right)\lim_{\lambda\to+\infty}\mathscr{L}^{\mathrm{L}}_{I_{\mathrm{agg}}}\left(\frac{\gamma}{P\zeta_1^{\mathrm{L}}(L)}\right), \tag{5}$$

where $\lim_{\lambda\to+\infty}\mathscr{L}^{\mathrm{L}}_{I_{\mathrm{agg}}}(s)$ *with* $s=\frac{\gamma}{P\zeta_1^{\mathrm{L}}(L)}$ *is given by*

$$\lim_{\lambda\to+\infty}\mathscr{L}^{\mathrm{L}}_{I_{\mathrm{agg}}}(s)=\exp\left(-2\pi\rho\int_0^{+\infty}\frac{\Pr^{\mathrm{L}}\left(\sqrt{u^2+L^2}\right)u}{1+\left(sP\zeta^{\mathrm{L}}\left(\sqrt{u^2+L^2}\right)\right)^{-1}}du\right)\exp\left(-2\pi\rho\int_0^{+\infty}\frac{\left[1-\Pr^{\mathrm{L}}\left(\sqrt{u^2+L^2}\right)\right]u}{1+\left(sP\zeta^{\mathrm{NL}}\left(\sqrt{u^2+L^2}\right)\right)^{-1}}du\right). \tag{6}$$

Proof: See Appendix A. ∎

between a BS and a UE is modeled as independently identical distributed (i.i.d.) Rayleigh fading [6–8].

It is important to note that it has been shown in [12] that the analysis of the following factors/models is not urgent, as they do not change the qualitative conclusions of this type of performance analysis in UDNs: *(i)* a non-Poisson distributed BS density, *(ii)* a BS density dependent transmission power, *(iii)* a more accurate multi-path modeling with Rician fading, and *(iv)* an additional modeling of correlated shadow fading. Thus, we will concentrate on presenting our most fundamental discoveries in this paper, and show the minor impacts of the above factors/models in the journal version of this work.

III. Main Result

In this section, we study the coverage probability performance and the network capacity in terms of the ASE.

A. The Coverage Probability

First, we investigate the coverage probability that the SINR of a typical UE at the origin o is above a threshold γ:

$$p^{\mathrm{cov}}(\lambda,\gamma)=\Pr\left[\mathrm{SINR}>\gamma\right], \tag{7}$$

where the SINR is computed by

$$\mathrm{SINR}=\frac{P\zeta(w)\,h}{I_{\mathrm{agg}}+P_{\mathrm{N}}}, \tag{8}$$

where h is the channel gain, which is modeled as an exponentially distributed random variable (RV) with a mean of one due to our consideration of Rayleigh fading mentioned in Subsection II-B, P and P_{N} are the BS transmission power and the additive white Gaussian noise (AWGN) power at each UE, respectively, and I_{agg} is the cumulative interference given by

$$I_{\mathrm{agg}}=\sum_{i:\,b_i\in\tilde{\Phi}\setminus b_o}P\beta_i g_i, \tag{9}$$

where b_o is the BS serving the typical UE, and b_i, β_i and g_i are the i-th interfering BS, the path loss from b_i to the typical UE and the multi-path fading channel gain associated with such link (also exponentially distributed RVs), respectively. Note that, in (9), only the BSs in $\tilde{\Phi}\setminus b_o$ inject effective interference into the network, where $\tilde{\Phi}$ denotes the set of the active BSs. In other words, the BSs in idle mode are not taken into account in the computation of I_{agg}.

Based on the general path loss model in (3) and the adopted UAS, in Theorem 1, we present our main result on the asymptotic performance of $p^{\mathrm{cov}}(\lambda,\gamma)$ in UDNs, i.e., $\lim_{\lambda\to+\infty} p^{\mathrm{cov}}(\lambda,\gamma)$.

From Theorem 1, we propose a new SINR invariance law in Theorem 2.

Theorem 2. *A new SINR invariance law: If* $L>0$ *and* $\rho<+\infty$*, then* $\lim_{\lambda\to+\infty} p^{cov}(\lambda,\gamma)$ *becomes a constant that is independent of* λ *in UDNs.*

Proof: See Appendix B. ∎

Theorem 2 dictates that *(i)* the *SINR decrease* effect due to the non-zero BS-to-UE antenna height difference L and *(ii)* the *SINR increase* due to the finite UE density ρ and the BS idle mode capability cancel out each other in realistic UDNs with $L>0$ and $\rho<+\infty$. Note that here the study on $\{L,\rho\}$ is finally complete because:

- The case of $L=0$ and $\rho=+\infty$ has been studied in [6–8], showing that $\lim_{\lambda\to+\infty} p^{\mathrm{cov}}(\lambda,\gamma)$ is a function of α_n^{L}.
- The case of $L>0$ and $\rho=+\infty$ has been studied in [10], showing that $\lim_{\lambda\to+\infty} p^{\mathrm{cov}}(\lambda,\gamma)=0$ as illustrated in Fig. 1.
- The case of $L=0$ and $\rho<+\infty$ has been studied in [11], showing that $\lim_{\lambda\to+\infty} p^{\mathrm{cov}}(\lambda,\gamma)=1$ as illustrated in Fig. 1.
- The case of $L>0$ and $\rho<+\infty$ is characterized by Theorem 2, which reflects the most practical SCN deployment among the above cases.

For Theorem 2, it is trivial to show that for a given $\{L,\rho\}$, $\lim_{\lambda\to+\infty} p^{\mathrm{cov}}(\lambda,\gamma)$ decreases as γ increases. This is because a higher SINR requirement naturally leads to a lower coverage probability. Thus, in Lemmas 3 and 4, we only address how $\lim_{\lambda\to+\infty} p^{\mathrm{cov}}(\lambda,\gamma)$ varies with L and ρ, respectively.

Lemma 3. *For a given* $\{\rho,\gamma\}$*,* $\lim_{\lambda\to+\infty} p^{cov}(\lambda,\gamma)$ *decreases as* L *increases.*

Proof: See Appendix C. ∎

Lemma 4. *For a given* $\{L,\gamma\}$*,* $\lim_{\lambda\to+\infty} p^{cov}(\lambda,\gamma)$ *decreases as* ρ *increases, according to a power law with respect to* ρ*.*

Proof: See Appendix D. ∎

The intuitions of Lemmas 3 and 4 are explained as follows,

- The signal power becomes bounded in UDNs due to the lower-bound on the BS-to-UE distance, as a UE cannot be closer than L to a BS. Moreover, a larger L implies a tighter bound on the signal power, which leads to the decrease of $\lim_{\lambda\to+\infty} p^{\mathrm{cov}}(\lambda,\gamma)$ addressed in Lemma 3.
- The interference power becomes bounded in UDNs due to the activation of a finite density of BSs (i.e., $\tilde{\lambda}$) to serve a finite density of UEs (i.e., ρ). Moreover, a larger ρ results in a larger $\tilde{\lambda}$, relaxing the bound on the interference power, which leads to the decrease of $\lim_{\lambda\to+\infty} p^{\mathrm{cov}}(\lambda,\gamma)$ addressed in Lemma 4. Such decrease follows a power law, because an HPPP distribution of UEs with ρ UEs/km^2 can be decomposed into ρ independent HPPP ones with 1 UEs/km^2, and the coverage criterion (7) should be satisfied for each one of these HPPP distributions, which yields a power law with respect to ρ.

B. The Area Spectral Efficiency

Next, we investigate the network capacity performance in terms of the area spectral efficiency (ASE) in bps/Hz/km^2, which is defined as [8]

$$A^{\mathrm{ASE}}(\lambda,\gamma_0)=\tilde{\lambda}\int_{\gamma_0}^{+\infty}\log_2(1+\gamma)\,f_{\Gamma}(\lambda,\gamma)\,d\gamma, \quad (11)$$

where γ_0 is the minimum working SINR in a practical SCN, and $f_{\Gamma}(\lambda,\gamma)$ is the probability density function (PDF) of the SINR γ observed at the typical UE for a particular value of λ. Based on the definition of $p^{\mathrm{cov}}(\lambda,\gamma)$ in (7) and the partial integration theorem shown in [9], (11) can be reformulated as

$$\begin{aligned}A^{\mathrm{ASE}}(\lambda,\gamma_0) \;=\; &\frac{\tilde{\lambda}}{\ln 2}\int_{\gamma_0}^{+\infty}\frac{p^{\mathrm{cov}}(\lambda,\gamma)}{1+\gamma}d\gamma\\ &+\tilde{\lambda}\log_2(1+\gamma_0)\,p^{\mathrm{cov}}(\lambda,\gamma_0). \quad (12)\end{aligned}$$

From (1), we have that $\tilde{\lambda}$ is a finite value since $\rho<+\infty$. Note that $\tilde{\lambda}$ also represents the frequency reuse factor in the considered SCN. Hence, $\tilde{\lambda}$ is used in the expression of $A^{\mathrm{ASE}}(\lambda,\gamma_0)$ because only the active BSs make an effective contribution to the ASE.

C. A New Capacity Scaling Law

From Theorem 5 and the expression of the ASE in (12), we propose a new capacity scaling law in Theorem 5.

The implication of this new capacity scaling law in Theorem 5 is profound, which will be discussed in the following.

Remark 1: As discussed in Section I, the implication of *the previous SINR invariance* found in [4] is that the network capacity should scale linearly as the BS density increases in a fully-loaded UDN (i.e., the frequency reuse factor is λ). Such conclusion gave us *a linear capacity scaling law* and showed **an optimistic future for 5G**.

Remark 2: The implication of our *new capacity scaling law*, which is a constant scaling law, is quite different. Specifically, the network densification should be *stopped* at a certain level for a given UE density ρ, because both the coverage probability and the network capacity will respectively reach a maximum constant value, thus showing **a practical future for 5G**. Any network densification beyond such level of BS density is a waste of both money and energy.

Remark 3: Recently some concerns about network capacity collapsing in UDNs have emerged, e.g., *the capacity crash* due to a non-zero BS-to-UE antenna height difference [10], or a bounded path loss in the near-field (NF) region [13], thus showing **a pessimistic future for 5G**. However, it should be noted that the above studies [10, 13] assumed an infinite UE density in UDNs, which is not realistic. Our new discovery on the *constant* capacity scaling law addresses such concerns.

- **Remark 3a:** The non-zero BS-to-UE antenna height difference precludes the existence of the NF effect, since the former one occurs when the height difference is in the order of meters [10], while the latter one emerges when the distance between a transmitter and a receiver is in the sub-meter region [13]. With this in mind, we can see that the NF effect will not occur in practical UDNs due to the non-zero BS-to-UE antenna height difference, unless we decide to lower the BS antenna height straight to the UE antenna height in the future [10]. But that would create new problems such as fast shadow fading [10] and the optimization of the BS antenna height.
- **Remark 3b:** As concluded in Theorem 5, the network capacity collapse will not happen in practical networks with a finite UE density. Even if the UE density is indeed infinite, the network capacity collapse can still be avoided by using time division multiple access (TDMA) or frequency division multiple access (FDMA) among groups of UEs with a finite density, so that a constant and decent network capacity can be achieved, as shown in Theorem 5. In other words, instead of letting the network capacity collapse with an infinite UE density in UDNs, our new capacity scaling law points out another way of *proactively choosing and serving a subset of UEs with a finite UE density* on each time/frequency resource block to optimize network performance, and thus completely mitigate the network capacity collapse.

Remark 4: Following the leads in **Remark 3b**, we further investigate (10) and observe that $\lim_{\lambda\to+\infty} A^{\mathrm{ASE}}(\lambda,\gamma_0)$ should be a concave function with regard to ρ, which implies an optimal UE density ρ^* for the TDMA/FDMA operation so as to maximize $\lim_{\lambda\to+\infty} A^{\mathrm{ASE}}(\lambda,\gamma_0)$. This is because

- Lemma 4 states that $\lim_{\lambda\to+\infty} p^{\mathrm{cov}}(\lambda,\gamma)$ decreases as ρ increases,
- while ρ also linearly scales the two terms in (10), and
- thus, there should exist an optimal UE density ρ^* that can maximize $\lim_{\lambda\to+\infty} A^{\mathrm{ASE}}(\lambda,\gamma_0)$ in (10), which removes the network capacity collapse as discussed in **Remark 3b**.

Actually, considering the general expression of the ASE with regard to λ in (12), we can make such optimization problem more general and formally propose **a BS scheduling problem**:

Theorem 5. *A constant capacity scaling law: If $L > 0$ and $\rho < +\infty$, then $\lim_{\lambda\to+\infty} A^{\mathrm{ASE}}(\lambda,\gamma_0)$ becomes a constant that is independent of λ in UDNs. In more detail, $\lim_{\lambda\to+\infty} A^{\mathrm{ASE}}(\lambda,\gamma_0)$ is given by*

$$\lim_{\lambda\to+\infty} A^{\mathrm{ASE}}(\lambda,\gamma_0) = \frac{\rho}{\ln 2}\int_{\gamma_0}^{+\infty} \frac{\lim_{\lambda\to+\infty} p^{\mathrm{cov}}(\lambda,\gamma)}{1+\gamma} d\gamma + \rho \log_2(1+\gamma_0) \lim_{\lambda\to+\infty} p^{\mathrm{cov}}(\lambda,\gamma_0), \tag{10}$$

where $\lim_{\lambda\to+\infty} p^{\mathrm{cov}}(\lambda,\gamma)$ is obtained from Theorem 1, and it is independent of λ in UDNs.

Proof: See Appendix E. ∎

For a given BS density λ, there exists an optimal UE density ρ^* that can maximize $A^{\mathrm{ASE}}(\lambda,\gamma_0)$, i.e.,

$$\begin{aligned} \underset{\rho}{\text{maximize}} \quad & A^{\mathrm{ASE}}(\lambda,\gamma_0) \\ \text{s.t.} \quad & 0 \le \rho \le \lambda. \end{aligned} \tag{13}$$

Note that the solution ρ^* to the BS scheduling problem (13) would also answer the fundamental question of *"what is the optimal frequency reuse factor $\tilde{\lambda}^*$ for a given BS density λ?"*, because ρ^* and $\tilde{\lambda}^*$ are linked by (1). Due to the page limit, we relegate the algorithm to solve (13) to our journal work.

Remark 5: Theorem 5 shows that $A^{\mathrm{ASE}}(\lambda,\gamma_0)$ in (12) reaches $\lim_{\lambda\to+\infty} A^{\mathrm{ASE}}(\lambda,\gamma_0)$ when $\lambda \to +\infty$. However, achieving such performance limit might be cost-inefficient due to the investment on the deployment of BSs as $\lambda \to +\infty$. Thus, we further propose **a BS deployment problem**: For a given UE density ρ, there exists an optimal BS density λ^* that can achieve a performance result of $A^{\mathrm{ASE}}(\lambda,\gamma_0)$ that is within a gap of ϵ-percent to $\lim_{\lambda\to+\infty} A^{\mathrm{ASE}}(\lambda,\gamma_0)$, i.e.,

$$\begin{aligned} \underset{\lambda}{\text{maximize}} \quad & 1 \\ \text{s.t.} \quad & \left| A^{\mathrm{ASE}}(\lambda,\gamma_0) - \lim_{\lambda\to+\infty} A^{\mathrm{ASE}}(\lambda,\gamma_0) \right| \le \epsilon. \end{aligned} \tag{14}$$

Note that the solution λ^* to the BS deployment problem (14) would also answer the fundamental question of *"how dense an UDN should be for a given UE density ρ?"*. It makes sense that such question and answer should depend on the UE density ρ. The intuition is that network densification should be *stopped* at λ^*, because the network capacity saturates at λ^* within a performance gap of ϵ-percent compared with $\lim_{\lambda\to+\infty} A^{\mathrm{ASE}}(\lambda,\gamma_0)$. Due to the page limit, we relegate the algorithm to solve (14) to our journal work.

IV. Simulation and Discussion

In this section, we investigate the SCN performance and use numerical results to validate the accuracy of our analysis. According to Tables A.1-3~A.1-7 of [5], we adopt the following parameters for the 3GPP Case: $\alpha^{\mathrm{L}} = 2.09$, $\alpha^{\mathrm{NL}} = 3.75$, $A^{\mathrm{L}} = 10^{-10.38}$, $A^{\mathrm{NL}} = 10^{-14.54}$, $P = 24$ dBm, $P_{\mathrm{N}} = -95$ dBm (including a noise figure of 9 dB at each UE).

A. Validation of the Coverage Probability Performance

In Fig. 2, we display the coverage probability for the 3GPP Case with $\gamma = 0$ dB and various values of ρ and L. In this figure, solid lines, markers, and dash lines represent analytical results, simulation results, and $\lim_{\lambda\to+\infty} p^{\mathrm{cov}}(\lambda,\gamma)$ derived in Theorem 1, respectively. Note that the analytical results of $p^{\mathrm{cov}}(\lambda,\gamma)$ in Fig. 2 are obtained from [10] with the use of $\tilde{\lambda}$. From this figure, we can observe that:

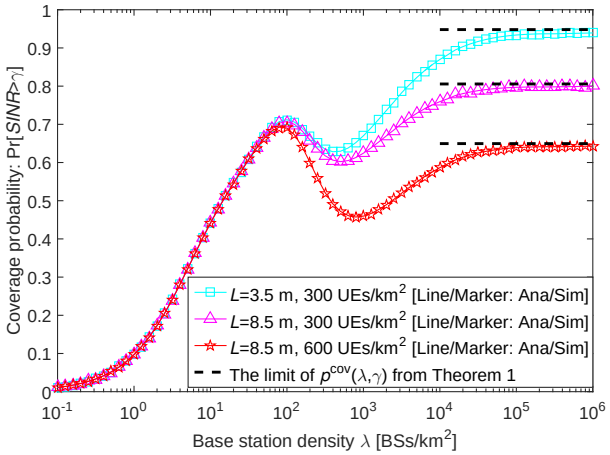
Coverage probability: Pr[SINR>γ]
Base station density λ [BSs/km²]
L=3.5 m, 300 UEs/km² [Line/Marker: Ana/Sim]
L=8.5 m, 300 UEs/km² [Line/Marker: Ana/Sim]
L=8.5 m, 600 UEs/km² [Line/Marker: Ana/Sim]
The limit of p^cov(λ,γ) from Theorem 1

Fig. 2. The coverage probability $p^{\mathrm{cov}}(\lambda,\gamma)$ vs. λ for the 3GPP Case with $\gamma = 0$ dB and various values of ρ and L.

- As already shown in Fig. 1, when the BS density is at around $\lambda \in [10^2, 10^3]$ BSs/km^2, $p^{\mathrm{cov}}(\lambda,\gamma)$ decreases with λ. This is due to the transition of a large number of interfere paths from NLoS to LoS, which accelerates the growth of the aggregate inter-cell interference [6, 8].
- When $\lambda \in [10^3, 10^5]$ BSs/km^2, $p^{\mathrm{cov}}(\lambda,\gamma)$ continuously increases thanks to the BS idle mode operations [11], i.e., the signal power continues increasing with the network densification, while the interference power becomes bounded, as only BSs with active UEs are turned on.
- When $\lambda > 10^5$ BSs/km^2, $p^{\mathrm{cov}}(\lambda,\gamma)$ gradually reaches its limit characterized by Theorem 1, which verifies the SINR invariance law in Theorem 2. Numerically speaking, the gap between the analytical results of $p^{\mathrm{cov}}(\lambda,\gamma)$ and those of $\lim_{\lambda\to+\infty} p^{\mathrm{cov}}(\lambda,\gamma)$ are less than 0.5 % for all of the investigated cases when $\lambda = 5\times10^5$ BSs/km^2, which validates the accuracy of Theorem 1.
- As shown in Fig. 2, when $\rho = 300$ UEs/km^2, the limit of $p^{\mathrm{cov}}(\lambda,\gamma)$ with $L = 3.5$ m is larger than that with $L = 8.5$ m, thus verifying Lemma 3.
- As shown in Fig. 2, when $L = 8.5$ m, the limit of

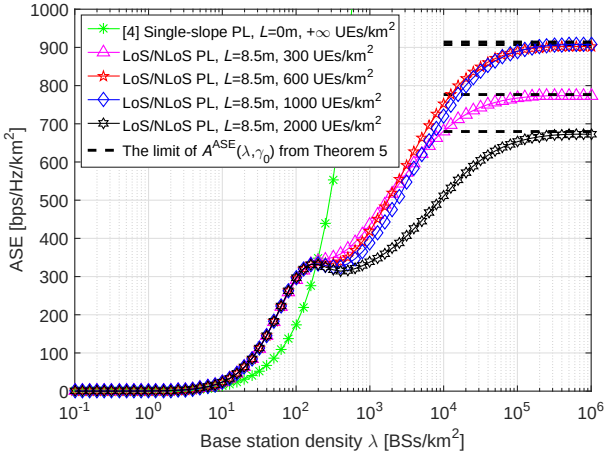
[4] Single-slope PL, L=0m, +∞ UEs/km²
LoS/NLoS PL, L=8.5m, 300 UEs/km²
LoS/NLoS PL, L=8.5m, 600 UEs/km²
LoS/NLoS PL, L=8.5m, 1000 UEs/km²
LoS/NLoS PL, L=8.5m, 2000 UEs/km²
The limit of A^ASE(λ,γ0) from Theorem 5
ASE [bps/Hz/km²]
Base station density λ [BSs/km²]

Fig. 3. The ASE $A^{\mathrm{ASE}}(\lambda, \gamma_0)$ vs. λ with $\gamma_0 = 0\,\mathrm{dB}$ for the 3GPP Case with $\gamma_0 = 0\,\mathrm{dB}$, $L = 8.5\,\mathrm{m}$ and various values of ρ.

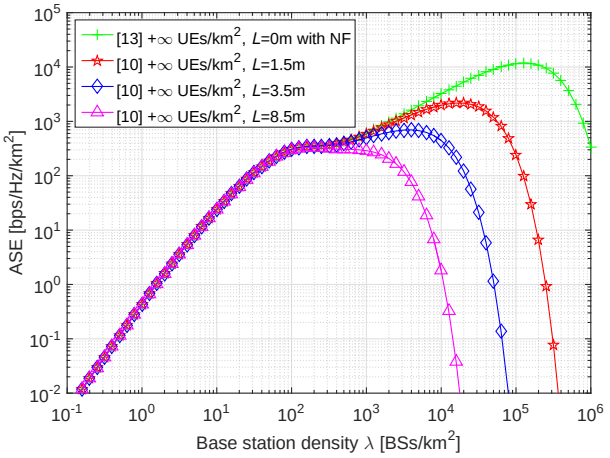

Fig. 4. The ASE $A^{\mathrm{ASE}}(\lambda, \gamma_0)$ vs. λ with $\gamma_0 = 0\,\mathrm{dB}$ for the 3GPP Case with $\rho = +\infty\,\mathrm{UEs/km^2}$ and various values of L.

$p^{\mathrm{cov}}(\lambda, \gamma)$ with $\rho = 300\,\mathrm{UEs/km^2}$ is 0.806, while that with $\rho = 600\,\mathrm{UEs/km^2}$ is 0.65, which equals to the square of 0.806, thus verifying Lemma 4.

B. Validation of the New Capacity Scaling Law

In Fig. 3, we plot the ASE results for the 3GPP Case with $\gamma_0 = 0\,\mathrm{dB}$, $L = 8.5\,\mathrm{m}$ and various values of ρ. Since $A^{\mathrm{ASE}}(\lambda, \gamma_0)$ is calculated from the results of $p^{\mathrm{cov}}(\lambda, \gamma)$ using (12), and because the analysis on $p^{\mathrm{cov}}(\lambda, \gamma)$ has been validated in Subsection IV-A, we only show the analytical results of $A^{\mathrm{ASE}}(\lambda, \gamma_0)$ in Fig. 3. From this figure, we can observe that:

- As discussed in **Remark 1**, due to its simplistic assumptions, *the linear capacity scaling law* [4] shows **an optimistic but unrealistic future for 5G UDNs** in Fig. 3.
- *The constant capacity scaling law* in Theorem 5 is validated for UDNs with a non-zero L and a finite ρ, showing **a practical future for 5G UDNs** in Fig. 3.
- For a given λ, e.g., $\lambda = 10^5\,\mathrm{BSs/km^2}$, it is interesting to see that $A^{\mathrm{ASE}}(\lambda, \gamma_0)$ is indeed a concave function of ρ and it achieves its maximum value when $\rho \in [600, 1000]\,\mathrm{UEs/km^2}$, which justify the BS scheduling problem (13) addressed in **Remark 4**.
- For a given ρ, e.g., $\rho = 300\,\mathrm{UEs/km^2}$, the value of $A^{\mathrm{ASE}}(\lambda, \gamma_0)$ saturates as $\lambda \to +\infty$, which justifies the BS deployment problem (14) addressed in **Remark 5**.

C. Network Capacity Collapsing: A Valid Problem or Not

In this subsection, we investigate the network capacity collapsing phenomenon and explain why our discovered constant capacity scaling law can completely mitigate such issue. As explained in **Remark 3**, network capacity collapsing only occurs with an infinite UE density in UDNs. Such analytical results are plotted in Fig. 4, where we show two capacity crashes respectively due to a non-zero BS-to-UE antenna height difference L [10], and a bounded path loss in the near-field (NF) region [13]. From this figure, we can observe that:

- As discussed in **Remark 3**, due to the assumption of $\rho = +\infty$, the network capacity collapsing phenomenon shows **a pessimistic but unrealistic future for 5G UDNs**.
- As discussed in **Remark 3a**, the network capacity collapsing due to a non-zero L precedes that caused by the NF effect, because the former one takes effect at a much larger distance scale than the latter one. **Thus, the network capacity collapsing due to the NF effect is avoided in practical UDNs due to the existence of a non-zero L.** The case of $L = 0$ is a completely uncharted territory that requires new channel measurements [10].
- As discussed in **Remark 3b**, even if $\rho = +\infty$, the network capacity collapsing due to a non-zero L can still be resolved by our discovered capacity scaling law with *proactively choosing and serving a subset of UEs* in a TDMA/FDMA manner. For example, in Fig. 4, when $L = 8.5\,\mathrm{m}$ and $\lambda = 10^4\,\mathrm{BSs/km^2}$, the ASE is merely around $1.78\,\mathrm{bps/Hz/km^2}$. However, if we randomly select and serve a subset of UEs with $600\,\mathrm{UEs/km^2}$, the ASE can be tremendously increased to around $752.3\,\mathrm{bps/Hz/km^2}$, as shown in Fig. 3. Thus, such network capacity collapsing due to a non-zero L is also not a problem thanks to our discovered capacity scaling law in this paper.

V. Conclusion

A new constant capacity scaling law has been discovered in UDNs. Such law has two profound implications. First, network densification should be *stopped* at a certain BS density for a given UE density, because the network capacity reaches a limit. Such BS density can be optimized by solving *the proposed BS deployment problem*, which also answers the fundamental question of *"how dense an UDN should be for a given UE density?"*. Second, the recent concerns about network capacity collapsing in UDNs can be resolved by our discovered capacity scaling law with *proactively choosing and serving a subset of UEs* in a TDMA/FDMA manner. Such UE density can be optimized by solving *the proposed BS scheduling problem*.

Appendix A: Proof of Theorem 1

As $\lambda \to +\infty$, we have that $r \to 0$ and $w \to L$ in (2). Consequently, the path loss of this link should be dominantly

characterized by *the first-piece LoS path loss function* (i.e., $\zeta_1^{\mathrm{L}}(w)$), e.g., L is smaller than $d_1 = 67.75$ m of the 3GPP Case in practical SCNs [5], which supports the use of $\zeta_1^{\mathrm{L}}(w)$ in such case. Thus, $\lim_{\lambda\to+\infty} p^{\mathrm{cov}}(\lambda,\gamma)$ can be derived as

$$\begin{aligned}\lim_{\lambda\to+\infty} p^{\mathrm{cov}}(\lambda,\gamma) &= \lim_{\lambda\to+\infty} \Pr\left[\mathrm{SINR}>\gamma \,\middle|\, \zeta(w)=\zeta_1^{\mathrm{L}}(L)\right] \\ &\overset{(a)}{=} \lim_{\lambda\to+\infty} \Pr\left[\frac{P\zeta_1^{\mathrm{L}}(L)\,h}{I_{\mathrm{agg}}+P_{\mathrm{N}}}>\gamma\right] \\ &= \lim_{\lambda\to+\infty} \Pr\left[h>\frac{(I_{\mathrm{agg}}+P_{\mathrm{N}})\,\gamma}{P\zeta_1^{\mathrm{L}}(L)}\right], \qquad (15)\end{aligned}$$

where (8) is plugged into the step (a) of (15). Considering that the complementary cumulative distribution function (CCDF) of h gives $\Pr[h > x_1 + x_2] = \exp(-x_1)\exp(-x_2)$ and with some mathematical manipulations, we can arrive at (5).

Then, we can further derive $\mathscr{L}_{I_{\mathrm{agg}}}^{\mathrm{L}}(s)$ with $s = \frac{\gamma}{P\zeta_1^{\mathrm{L}}(L)}$ as

$$\begin{aligned}&\mathscr{L}_{I_{\mathrm{agg}}}^{\mathrm{L}}(s) \\ &= \mathbb{E}_{[I_{\mathrm{agg}}]}\left\{\exp(-sI_{\mathrm{agg}})\right\} \\ &\overset{(a)}{=} \mathbb{E}_{\left[\tilde{\Phi}\setminus b_o,\{\beta_i\},\{g_i\}\right]}\left\{\exp\left(-s\sum_{i\in\Phi/b_o} P\beta_i g_i\right)\right\} \\ &\overset{(b)}{=} \exp\left(-2\pi\tilde{\lambda}\int_0^{\infty}\left(1-\mathbb{E}_{[g]}\left\{\exp\left(-sP\beta\left(\sqrt{u^2+L^2}\right)g\right)\right\}\right)u\,du\right) \\ &\overset{(c)}{=} \exp\left(-2\pi\tilde{\lambda}\int_0^{+\infty}\frac{\Pr^{\mathrm{L}}\left(\sqrt{u^2+L^2}\right)u}{1+\left(sP\zeta^{\mathrm{L}}\left(\sqrt{u^2+L^2}\right)\right)^{-1}}du\right) \\ &\quad\times\exp\left(-2\pi\tilde{\lambda}\int_0^{+\infty}\frac{\left[1-\Pr^{\mathrm{L}}\left(\sqrt{u^2+L^2}\right)\right]u}{1+\left(sP\zeta^{\mathrm{NL}}\left(\sqrt{u^2+L^2}\right)\right)^{-1}}du\right), \qquad (16)\end{aligned}$$

where the step (a) of (16) comes from (9), the step (b) of (16) is obtained from Campbell's theorem [4], and $\mathbb{E}_{[g]}\{\exp(-sxg)\} = \frac{1}{1+sx}$ is plugged into the step (c) of (16) and interference from both LoS and NLoS paths are considered therein. Finally, from (1), we have that $\lim_{\lambda\to+\infty}\tilde{\lambda} = \rho$, which yields the result of $\lim_{\lambda\to+\infty}\mathscr{L}_{I_{\mathrm{agg}}}^{\mathrm{L}}\left(\frac{\gamma}{P\zeta_1^{\mathrm{L}}(L)}\right)$ in (6) and thus concludes our proof.

Appendix B: Proof of Theorem 1

Due to the page limit, here we only provide the key steps of the proof as follows. The proof is mainly consisted of two parts, where *(i)* in (5), $\exp\left(-\frac{P_{\mathrm{N}}\gamma}{P\zeta_1^{\mathrm{L}}(L)}\right)$ is a function of L and γ. Note that in reality it is a value very close to 1 because usually we have $P\zeta_1^{\mathrm{L}}(L) \gg P_{\mathrm{N}}$, and *(ii)* in (6), $\lim_{\lambda\to+\infty}\mathscr{L}_{I_{\mathrm{agg}}}^{\mathrm{L}}\left(\frac{\gamma}{P\zeta_1^{\mathrm{L}}(L)}\right)$ is a function of L, ρ and γ.

Appendix C: Proof of Lemma 3

Due to the page limit, here we only provide the key steps of the proof as follows. The proof is mainly consisted of two parts, where for a given $\{\rho,\gamma\}$, *(i)* in (5), we have that $\exp\left(-\frac{P_{\mathrm{N}}\gamma}{P\zeta_1^{\mathrm{L}}(L)}\right)$ decreases as L increases, and *(ii)* in (6), we have that $s = \frac{\gamma}{P\zeta_1^{\mathrm{L}}(L)}$ increases as L increases, and L quickly becomes irrelevant in the integrals of (6) because L appears in the term $\sqrt{u^2+L^2}$ and the integrals are performed on u toward $u = +\infty$, which leads to the conclusion that $\lim_{\lambda\to+\infty}\mathscr{L}_{I_{\mathrm{agg}}}^{\mathrm{L}}(s)$ is a decreasing function of s, and thus L. Note that Lemma 3 supports the recommendation of lowering the BS antenna height to achieve performance improvement [10].

Appendix D: Proof of Lemma 4

From (6), we can see that $\lim_{\lambda\to+\infty}\mathscr{L}_{I_{\mathrm{agg}}}^{\mathrm{L}}\left(\frac{\gamma}{P\zeta_1^{\mathrm{L}}(L)}\right)$ ranges from 0 to 1 and it is a decreasing power function of ρ. For example, if we double or triple the value of ρ, $\lim_{\lambda\to+\infty} p^{\mathrm{cov}}(\lambda,\gamma)$ will decrease by a factor of 4 or 9.

Appendix E: Proof of Theorem 5

Due to the page limit, here we only provide the key steps of the proof as follows. As $\lambda \to +\infty$, the ASE in (12) approaches a limit that is independent of λ. This is because *(i)* from Theorem 1, we can get that both $\lim_{\lambda\to+\infty} p^{\mathrm{cov}}(\lambda,\gamma)$ and $\lim_{\lambda\to+\infty} p^{\mathrm{cov}}(\lambda,\gamma_0)$ are independent of λ, and *(ii)* from (1) we have that $\lim_{\lambda\to+\infty}\tilde{\lambda} = \rho$, which is also independent of λ and has been plugged into (10). Therefore, $\lim_{\lambda\to+\infty} A^{\mathrm{ASE}}(\lambda,\gamma_0)$ is independent of λ as $\lambda \to +\infty$, which completes our proof.

References

[1] 3GPP, "TR 36.872: Small cell enhancements for E-UTRA and E-UTRAN - Physical layer aspects," Dec. 2013.

[2] D. López-Pérez, M. Ding, H. Claussen, and A. Jafari, "Towards 1 Gbps/UE in cellular systems: Understanding ultra-dense small cell deployments," *IEEE Communications Surveys Tutorials*, vol. 17, no. 4, pp. 2078–2101, Jun. 2015.

[3] S. Lee and K. Huang, "Coverage and economy of cellular networks with many base stations," *IEEE Communications Letters*, vol. 16, no. 7, pp. 1038–1040, Jul. 2012.

[4] J. Andrews, F. Baccelli, and R. Ganti, "A tractable approach to coverage and rate in cellular networks," *IEEE Transactions on Communications*, vol. 59, no. 11, pp. 3122–3134, Nov. 2011.

[5] 3GPP, "TR 36.828: Further enhancements to LTE Time Division Duplex for Downlink-Uplink interference management and traffic adaptation," Jun. 2012.

[6] X. Zhang and J. Andrews, "Downlink cellular network analysis with multi-slope path loss models," *IEEE Transactions on Communications*, vol. 63, no. 5, pp. 1881–1894, May 2015.

[7] T. Bai and R. Heath, "Coverage and rate analysis for millimeter-wave cellular networks," *IEEE Transactions on Wireless Communications*, vol. 14, no. 2, pp. 1100–1114, Feb. 2015.

[8] M. Ding, P. Wang, D. López-Pérez, G. Mao, and Z. Lin, "Performance impact of LoS and NLoS transmissions in dense cellular networks," *IEEE Transactions on Wireless Communications*, vol. 15, no. 3, pp. 2365–2380, Mar. 2016.

[9] M. D. Renzo, W. Lu, and P. Guan, "The intensity matching approach: A tractable stochastic geometry approximation to system-level analysis of cellular networks," *IEEE Transactions on Wireless Communications*, vol. 15, no. 9, pp. 5963–5983, Sep. 2016.

[10] M. Ding and D. López-Pérez, "Please Lower Small Cell Antenna Heights in 5G," *IEEE Globecom 2016*, pp. 1–6, Dec. 2016.

[11] M. Ding, D. López-Pérez, G. Mao, and Z. Lin, "Study on the idle mode capability with LoS and NLoS transmissions," *IEEE Globecom 2016*, pp. 1–6, Dec. 2016.

[12] M. Ding and D. López-Pérez, "On the performance of practical ultra-dense networks: The major and minor factors," *The IEEE Workshop on Spatial Stochastic Models for Wireless Networks (SpaSWiN) 2017*, pp. 1–8, May 2017. [Online]. Available: https://arxiv.org/abs/1701.07964

[13] J. Liu, M. Sheng, L. Liu, and J. Li, "How Dense is Ultra-Dense for Wireless Networks: From Far- to Near-Field Communications," *arXiv:1606.04749 [cs.IT]*, Jun. 2016.